Published in final edited form as:
*Int J Dev Neurosci*. 2013 November ; 31(7): . doi:10.1016/j.ijdevneu.2013.06.004.

# Quantitative evaluation of brain development using anatomical MRI and diffusion tensor imaging☆

**Kenichi Oishi**[a,*], **Andreia V. Faria**[a], **Shoko Yoshida**[a], **Linda Chang**[b], and **Susumu Mori**[b,c]

[a]The Russell H. Morgan Department of Radiology and Radiological Science, The Johns Hopkins University School of Medicine, Baltimore, MD, USA

[b]Neuroscience and Magnetic Resonance Research Program, John A. Burns School of Medicine, University of Hawaii at Manoa, Honolulu, HI, USA

[c]F.M. Kirby Research Center for Functional Brain Imaging, Kennedy Krieger Institute, Baltimore, MD, USA

## Abstract

The development of the brain is structure-specific, and the growth rate of each structure differs depending on the age of the subject. Magnetic resonance imaging (MRI) is often used to evaluate brain development because of the high spatial resolution and contrast that enable the observation of structure-specific developmental status. Currently, most clinical MRIs are evaluated qualitatively to assist in the clinical decision-making and diagnosis. The clinical MRI report usually does not provide quantitative values that can be used to monitor developmental status. Recently, the importance of image quantification to detect and evaluate mild-to-moderate anatomical abnormalities has been emphasized because these alterations are possibly related to several psychiatric disorders and learning disabilities. In the research arena, structural MRI and diffusion tensor imaging (DTI) have been widely applied to quantify brain development of the pediatric population. To interpret the values from these MR modalities, a “growth percentile chart,” which describes the mean and standard deviation of the normal developmental curve for each anatomical structure, is required. Although efforts have been made to create such a growth percentile chart based on MRI and DTI, one of the greatest challenges is to standardize the anatomical boundaries of the measured anatomical structures. To avoid inter- and intra-reader variability about the anatomical boundary definition, and hence, to increase the precision of quantitative measurements, an automated structure parcellation method, customized for the neonatal and pediatric population, has been developed. This method enables quantification of multiple MR modalities using a common analytic framework. In this paper, the attempt to create an MRI- and a DTI-based growth percentile chart, followed by an application to investigate developmental abnormalities related to cerebral palsy, Williams syndrome, and Rett syndrome, have been introduced. Future directions include multimodal image analysis and personalization for clinical application.



*Corresponding author at: The Russell H. Morgan Department of Radiology and Radiological Science, The Johns Hopkins University School of Medicine, 217D Traylor Building, 720 Rutland Avenue, Baltimore, MD 21205, USA. Tel.: +1 410 502 3553; fax: +1 410 614 1948. koishi@mri.jhu.edu, sentankobe@yahoo.co.jp (K. Oishi).

**Keywords**

Neonate; Pediatric; Magnetic resonance imaging; Diffusion tensor imaging; Normalization; Quantification; Brain atlas

## 1. Introduction: quantitative image analysis for the pediatric population

Quantitative measurements play essential roles in the clinical evaluation of human fetal and neonatal development. During pregnancy, fetuses are measured for the diameter of the gestational sac, crown-rump length, biparietal length, and femur length. After birth, neonates are measured for their height, body weight, and head circumference. The height and body weight are periodically measured throughout childhood to monitor developmental status. These measurements are typically interpreted based on a growth percentile chart. The measured values that are outside two standard deviations of the normal developmental curves are identified as a “developmental abnormality” and further evaluations are warranted to identify the cause of the abnormality.

The human brain is an organ that develops non-linearly from the fetal stage to adolescence (Bennett and Baird, 2006; Giedd et al., 1999). The development is structure-specific and the growth rate of each structure differs depending on the age of the subject (Kinney et al., 1988; Wiggins, 1986; Yakovlev and Lecours, 1967). Therefore, an imaging modality with a clear contrast that enables the identification of various anatomical structures in the brain is required for the structure-specific evaluation of the developmental status. Magnetic resonance imaging (MRI) is often used for this evaluation because of the high spatial resolution and contrast (Berman et al., 2005; Cascio et al., 2007; Dubois et al., 2006, 2008; Gao et al., 2009; Huppi et al., 1998; Shaw et al., 2008). The sensitivity and specificity to detect developmental brain abnormalities is often higher with MRI than with other neuroimaging modalities (Arnould et al., 2004; Inder et al., 2003; van Wezel-Meijler et al., 2011). The non-invasiveness and the lack of ionizing radiation of MRI are ideal for the evaluation of fetuses and individuals during early developmental stages, since they are more vulnerable to radiation then (Pearce et al., 2012). In extreme cases, such as xeroderma pigmentosum, which is a genetic disorder of DNA repair that causes brain atrophy in childhood, MRI is exclusively used (Ueda et al., 2012) because imaging modalities using radiation, such as X-ray computed tomography, must be avoided.

Currently, radiologists routinely read clinical MRIs qualitatively, based on their a priori knowledge and experience about the changes in size and contrast throughout brain development. Although the qualitative image reading is useful for the clinical decision-making, it does not provide quantitative values that can be used to monitor developmental status. If the volumes of particular anatomical structures can be quantified, clinicians can interpret the development of particular volumes with regard to the age-appropriate growth charts, similar to those used for body height and weight. Moreover, recent advancements in the technological aspects of image modalities and the research findings from precise image analyses suggest the importance of image quantification to detect and evaluate subtle anatomical abnormalities, particularly in relation to neurodevelopmental abnormalities, as well as several psychiatric disorders and learning disabilities (Arzoumanian et al., 2003; Clouchoux and Limperopoulos, 2012; Eikenes et al., 2011; Lindqvist et al., 2011; Mathur et al., 2010; Ment et al., 2009; Rose et al., 2009; Skranes et al., 2007, 2009; Soria-Pastor et al., 2009; Vangberg et al., 2006).

There are two categories of images to be quantified. The first category is a qualitative image with relative intensities, in which the intensity itself has an arbitrary scale, such as

conventional structural MRI (e.g., T1- and T2-weighted images). To quantify these qualitative images, the image contrast must be converted to quantitative values. For example, morphological information, normalized intensity, or values derived from an intensity histogram, such as skewness and kurtosis, are extracted (Jack et al., 2001). Among these data, morphological information is often the target of analysis, in which the volume or shape of the location of interest is quantified (Chang et al., 2004; Gimenez et al., 2006; Lodygensky et al., 2008; Silk and Wood, 2011). Another category is a quantitative image in which the intensity of each voxel represents useful information. The T2 map, which is calculated from multiple anatomical MRIs with different echo times, and diffusion tensor imaging (DTI), which is calculated from multiple diffusion-weighted images and a non-diffusion weighted image, are quantitative MRI methods that are widely accepted in pediatric studies (Gilmore et al., 2007; Neil et al., 1998). The T2 map is used to evaluate myelination of the brain (Beaulieu et al., 1998; Ding et al., 2004, 2008; Dyakin et al., 2010; Ferrie et al., 1999; Miot-Noirault et al., 1997; Miot et al., 1995). DTI provides quantitative scalar images with rich anatomical information (Basser et al., 1994; Beaulieu and Allen, 1994; Berman et al., 2005; Conturo et al., 1996; Hsu and Mori, 1995; McKinstry et al., 2002; Miller et al., 2002; Mori et al., 2001; Mukherjee et al., 2002; Neil et al., 1998; Pierpaoli et al., 1996; Ulug and van Zijl, 1999), based on directionality of water diffusion that coincides with the orientation of ordered structures. The fractional anisotropy (FA) (Pierpaoli and Basser, 1996; Pierpaoli et al., 1996), which represents the degree of anisotropy of the diffusion, and the mean diffusivity (MD), which represents the magnitude of diffusion, are commonly used scalar measurements. When these quantitative images are analyzed, the intensity itself is the target of interest.

Both structural MRI and DTI have been widely applied to quantify brain development in the pediatric population. Similar to staining methods used for histopathology, each modality includes different types of information, all of which represent the different background anatomy. Past studies have aimed to create the “growth percentile chart,” which is necessary for interpretation, based on the modality used and on study-specific database. Although there is an ongoing effort to collect pediatric images from multiple institutes to serve as an open-access database (2012; Almli et al., 2007; Evans, 2006; Waber et al., 2007), there is no standardized growth percentile chart, created by using a common analytic framework for both structural MRI and DTI, available for public use. This lack of a standardized growth percentile chart is a current bottleneck that restricts the widespread use of image quantification in the pediatric population, especially for clinical use with which pediatricians must make clinical decisions for each patient without a normal control group.

One of the greatest challenges in the creation of a growth percentile chart is to standardize the anatomical boundaries of the measured structures. When measuring the body weight or head circumference, the names of the measurements themselves carry well-standardized meanings, with little ambiguity. However, the definition of the anatomical boundary of each brain structure is often ambiguous; for example, the reported normal hippocampal volumes differ by up to 2.5-fold depending on the definitions of the boundary that is manually drawn to measure the volume (Boccardi et al., 2011 ).To avoid inter-institutional, inter-reader, and intra-reader variability of the anatomical boundary definitions, and thus, to increase the precision of the quantitative measurements, computer-assisted automated segmentation of the brain has been applied to adult brain MRI (Collins et al., 1995; Fischl et al., 2002; Heckemann et al., 2006; Maldjian et al., 2003; Mallar Chakravarty et al., 2012; Mori et al., 2008; Oishi et al., 2008, 2009; Tzourio-Mazoyer et al., 2002). Yet, an automated method to define the anatomical boundaries of brain structural MRI and DTI in various developmental stages had not been fully developed until recently (Shi et al., 2009, 2010).

In this article, we will introduce the various methods to quantify qualitative image (structural MRI) and quantitative image (DTI) data about the developing brain, using a common analytic framework. We will also provide some research data to demonstrate normal brain development, and how we can apply these quantitative approaches to investigate developmental abnormalities associated with various diseases.

## 2. Methods to quantify information from images: voxel- and atlas-based quantification

The simplest and the most established method for image quantification is a region-of-interest (ROI)-based method, in which a selected set of ROIs is placed on the structures to retrieve and quantify the values (e.g., volume of the structure). This approach is suitable when investigating the normal developmental pattern of selected anatomical structures, such as the hippocampus (Jacob et al., 2011), or when targeting a specific disease with a developmental abnormality in known anatomical structures. However, if there is no clear a priori knowledge, or if multiple diseases with different distributions of anatomical abnormalities are evaluated, arbitrarily selected ROIs are not adequate. To explore the unknown effects of a particular disease, or to quantify the developmental status of the pediatric population, including a wide range of diseases, whole-brain analysis is the method of choice.

There are several approaches to whole-brain analysis. If information with high spatial resolution is needed, a voxel-based analysis (VBA) can be performed, in which each voxel is regarded as one ROI. For a group analysis, each voxel at the same anatomical location must be identified across subjects. To fulfill this requirement, all MRIs are mathematically transformed to a common space. This common space serves as the basis for common anatomical locations on multiple MRIs to allow voxel-by-voxel analysis. VBA has been widely used in the pediatric population in children over four years old (Wilke and Holland, 2003; Wilke et al., 2002, 2003), and, more recently, for even younger populations (Gimenez et al., 2008). Because of the small size of the voxels, VBA could potentially provide information about changes in confined anatomical areas or about a small portion of a structure. The drawbacks are related to the small size (thus inherently noisy) and the large number of ROIs to cover the entire brain, which would lead to lower statistical power after correction for multiple comparisons. VBA is not suitable for detecting small but widespread change in the brain (Davatzikos, 2004). In addition, there are residual misregistrations after image transformations, which might affect the image quantification. For the DTI analysis, the tract-based spatial statistics (TBSS) method could reduce the effect of misregistration and low signal-to-noise-ratio (Ball et al., 2010; Smith et al., 2006), although the volume of the brain structures cannot be quantified by this method.

The simplest approach to ameliorate these issues related to VBA is to enlarge the size of the ROI. For example, isotropic spatial filtering is commonly used to enlarge the ROI. The larger the ROI, the higher the signal-to-noise ratio, which leads to a higher statistical power. The larger ROI can also reduce the effect of misregistration. As a result, in general, a large ROI is suitable to detect small but widespread changes in the brain. There are many ways of grouping voxels to shape ROIs, and the choice depends on scientific or clinical interests. For the evaluation of brain development, the goal is to evaluate the developmental pattern of each anatomical structure. Therefore, the contour of each ROI should follow the boundary of the anatomical structures. If there is a pre-segmented set of ROIs that covers the entire brain in the common space, which is often called a “parcellation map,” this can be transformed to the original image to quantify the volume of each anatomical structure, as well as to measure the intensities of the quantitative images (Aljabar et al., 2009; Collins et al., 1995; Heckemann et al., 2006, 2010; Jia et al., 2012; Joshi et al., 2004; Klein and Hirsch, 2005;

Maldjian et al., 2003; Mori et al., 2008; Oishi et al., 2008, 2009; Tzourio-Mazoyer et al., 2002; Warfield et al., 2004). More recently, a multi-atlas approach has emerged, in which multiple brain atlases with heterogeneous anatomies are mapped to the target image. The parcellation results from these atlases could be combined either with equal weighting or with weighting based on various types of information, such as nonlocal or local anatomical similarity between the atlas and the image to be parcellated. The multi-atlas approach has the potential to accommodate the large anatomical variability encountered in clinical images and to deliver a high level of parcellation accuracy (Aljabar et al., 2009; Artaechevarria et al., 2009; Fischl et al., 2002; Heckemann et al., 2006; Klein and Hirsch, 2005; Langerak et al., 2010; Mori et al., 2013; Rousseau et al., 2011; Tang et al., 2013; van Rikxoort et al., 2010; Warfield et al., 2004; Wu et al., 2007; Yushkevich et al., 2009). Statistical analysis can be performed in a structure-by-structure manner, which is called "atlas-based analysis (ABA)," in contrast to the voxel-by-voxel manner in VBA. The parcellation map used for the ABA can be considered a standard definition of brain structures to achieve a high precision in image quantification, which is an essential step in establishing a standard growth percentile chart that can be shared by multiple institutions.

Since each parcel of the parcellation map contains many voxels, there is less information about anatomical localization than is provided by VBA. For example, if the atrophy is restricted to a part of the anatomical structure (e.g., anterior portion of the hippocampus), but the ROI includes the entire structure (e.g., whole hippocampus), the localized atrophy might be misunderstood as an atrophy of the entire hippocampus, or the atrophy might be diluted and be undetectable by ABA (Oishi et al., 2011b). VBA and ABA observe the brain from very different granularity levels (VBA: typically more than 100,000 voxels; ABA: typically 30–200 structures) and are complementary to each other for a multi-modal whole brain analysis.

## 3. MRI and DTI atlases for neonatal and pediatric image analyses

For the whole-brain analysis, a common space that serves as the basis of common anatomical locations is required. One simple option is to use a single-subject image or a population-averaged image as a template to transform all images. For adult brains, there are several standardized atlases that can be used as a template, such as ICBM atlases (http://www.loni.ucla.edu/ICBM/Downloads/Downloads_Atlases.shtml) and the Talairach atlas (Talairach and Tournoux, 1988). The advantage of using these standardized atlases is that it enables the reporting of research findings in a standardized coordinate system, which is convenient for comparing data from different studies. There are several brain parcellation maps created on these standardized atlases that are available for the ABA (Collins et al., 1995; Maldjian et al., 2003; Tzourio-Mazoyer et al., 2002). However, if there are substantial differences in contrast, shape, or size between the atlas and the images, the transformation accuracy might be poor (Lobel et al., 2009; Muzik et al., 2000; Wilke et al., 2003). Therefore, for pediatric studies with different age groups, or when there is a considerable amount of anatomical variation, study-specific templates, which are customized to fit to the anatomical features of the study population, are often employed (Wilke et al., 2008). Whole-brain analysis for the pediatric population is often performed for morphometric analysis based on VBA. ABA is less common because study-specific templates usually do not have a parcellation map.

To create a standardized atlas for the pediatric population that could serve as a common language by which to compare results from multiple institutes and researchers, the target age-range should be specified to increase the transformation accuracy. This is especially important for the younger population since the contrast in anatomical MRI changes rapidly during brain development, mainly due to the ongoing myelination process (Barkovich et al.,

1988; Huppi et al., 1998; van der Knaap and Valk, 1990). Moreover, the gray and white matter contrast of anatomical MRIs of the younger population, especially children under one year old, is not as clear as that seen in the older pediatric population. The poor contrast is disadvantageous for whole-brain analyses that use image transformation, since the transformation algorithm usually uses contrasts to guide the co-registration of identical anatomical structures from the two images. Therefore, accurate anatomical co-registration is difficult in brain areas that have little or no MRI contrast between different tissues. One solution is to incorporate DTI to guide the transformation (Ceritoglu et al., 2009; Oishi et al., 2009; Studholme, 2008). DTI is capable of depicting well-aligned structures, such as axonal bundles, and hence provides rich contrast within the white matter, even for the neonatal brain with less myelination (Fig. 1); in fact, most of the white matter structures seen in the adult brain with DTI have already been established in the neonatal brain and can be visualized by DTI (Huang et al., 2006; Zhang et al., 2007). This motivated us to create co-registered MRI-and DTI-based, age-specific atlases, with parcellation maps, for the pediatric population (Fig. 2). Compared to a transformation based on T2-weighted contrast, DTI-based contrast achieved higher accuracy for the co-registration of white matter structures (Oishi et al., 2011c, 2012). The MRI/DTI atlas for neonates, and for 18-, and 24-month-olds is now available through the website (http://cmrm.med.jhmi.edu/).

While a population-averaged template is one of the most widely used templates that represents the averaged anatomy of the population of interest, image averaging leads to blurring of anatomical definition, which could interfere with the higher-order diffeomorphic deformation that is used for accurate normalization. Single-subject atlases do not have this blurring problem, but the anatomy is biased, which could adversely affect the accuracy of subsequent quantification, as well as the detection of abnormalities. There are several strategies to improve the atlas for accurate identification of brain anatomical structures. The use of a Bayesian template is one of the solutions, in which averaged features of the population are included, while maintaining the sharp contrast comparable to that of the single-subject image (Zhang et al., 2011b).

## 4. Exploring the developmental pattern of normal brains

Although the MRI/DTI images are transformed to the atlas for VBM, or the parcellation map in the atlas space is transformed to the individual MRI/DTI images for ABA, the quantified values must be interpreted based on a “growth percentile chart,” which would provide new ways to evaluate MRI/DTI. Namely, the quantified values of various brain regions of normal brains (e.g., volume, FA, or MD) would enable researchers to conduct statistical comparisons between diagnostic groups, as well as to investigate the relationships between brain anatomy and neurologic symptoms and future neurologic outcomes. This method is potentially useful for detecting previously hard-to-define abnormalities in each individual. In the following sections, actual data are introduced from our studies to demonstrate the efficacy of the quantitative approaches.

### 4.1. Babies (37–53 post-menstrual weeks)

The ABA was applied to analyze 22 DTIs and 13 T1- and T2-maps from healthy full-term babies (Oishi et al., 2011c). The babies were scanned without sedation, while they were sleeping. They were comfortably placed in a vacuum stabilizer, modified for size. The motion was monitored by the research staff, and re-scanned when motions were observed. Approximately half the babies were re-scanned more than once. Neonatal ear covers were used to attenuate sounds emitted from the MR system. The scans were performed on a 3T scanner with 12-channel head array coil, using single-shot echo planar imaging (EPI) with SENSE (reduction factor of 2) acquisition for DTI, double-echo fast spin echo to calculate the T2 map, and 3D inversion recovery to calculate the T1 map. For DTI, diffusion

weighting was applied along 12 axes with $b = 1000$ s/mm$^2$. Tensor calculation was performed on DTIstudio (Jiang et al., 2006), in which an automated outlier rejection method, based on modified RESTORE (Chang et al., 2005; Li et al., 2010) to remove corrupted data points, is implemented. The resolution was 1.0 mm × 1.0 mm × 2.0 mm for DTI and 1.7 mm × 1.7 mm × 5 mm for T1 and T2 maps. The total imaging time was approximately 20min. There was a general trend toward decreasing T1, T2, and MD, and increasing FA with age, with a structure-specific maturation pattern. Namely, there was a posterior-to-anterior and a central-to-peripheral direction of maturation. In Fig. 3, four representative areas with markedly different slopes and intercepts are shown to provide an idea about the relationships between data variability and effect size.

### 4.2. Pediatric population

There is a biphasic development of the brain – rapid growth in the first two years of life, followed by slower and subtler developmental changes. The ABA was used to investigate this later developmental change detected by DTI (Faria et al., 2010). Data from a total of 35 subjects from our pediatric database, open to public use (www.lbam.med.jhmi.edu) (Hermoye et al., 2006), were used. Images were acquired using a SENSE head coil (reduction factor of 2.5) on a 1.5 T scanner. An eight-element arrayed radio frequency coil, converted to a six-channel to be compatible with the six-channel receiver system, was used (detailed in Hermoye et al. (2006)). A single-shot EPI was used, with diffusion gradients applied in 32 directions and $b = 700$ s/mm$^2$. The resolution was 2.3 mm × 2.3 mm × 2.3 mm for individuals between two and five years old and 2.5 mm × 2.5 mm × 2.5 mm for older subjects. Tensor calculation was performed in DTIstudio. The ABA was performed in the original image space, by warping the anatomical parcellation map in the atlas space to the original MRI. In terms of volume, the ABA showed an age-dependent increase that was mostly uniform across the WM, although regions that are rich with projection fibers (e.g., the corona radiata, the internal capsule, the cerebral peduncle, and the corticospinal tract in the pons) tended to have higher age-dependent slopes, as well as $R^2$ values. There were no areas with decreasing volumes with age (Fig. 4).

The DTI analyses (Fig. 5) revealed an increase in FA with age in the WM, among which the brainstem, the thalamus, and the anterior limb of the internal capsules had the greatest age-dependent FA increase. In contrast, some cortical areas had age-dependent decreases in diffusivity measurements. The frontal WM showed a greater age-dependence than that in other regions.

### 4.3. Future directions: standardization of quantified values

Data standardization is one of the general requirements for clinical tests. The measured values are normalized to standardized units for inter-institutional comparison. Similarly, although the normal developmental database of MRI/DTI-derived parameters from a single scanner and protocol is useful for interpreting within-institute images, methods to standardize data from different scan protocols or scanners are necessary for generalization of research findings, and to create agreement about the detection of abnormalities of the brain anatomy. For anatomical MRI, the main problem stems from the scan-protocol-dependent differences in the intensity profile that creates contrast among the gray matter, white matter, and the cerebrospinal fluid. Therefore, intensity normalization is often used for volumetric analysis. Standardization of the DTI-derived parameters is more challenging, since numerous factors, such as the noise, *b*-value, voxel size, method used for tensor estimation, and more, may affect the results (Bammer et al., 2003; Farrell et al., 2007; Jones and Basser, 2004; Koay et al., 2006; Landman et al., 2007; Zhu et al., 2011). These factors must be well-controlled before the analysis. Investigation of the effect-size of these confounding factors and developing methods to reduce these effects are important future directions.

## 5. Detecting the effects of diseases and injuries

Once the growth percentile chart is established for quantitative image analysis, the next step is the application of the chart to detect various types of developmental abnormalities related to diseases. In the following sections, examples of the ABA applied to a spectrum of diseases, such as cerebral palsy and genetic conditions, including Williams and Rett syndromes, are demonstrated.

### 5.1. Cerebral palsy

Cerebral palsy is the most common chronic motor disorder of childhood, which includes a number of etiologies and clinical presentations. Identifying and understanding the factors responsible for the variability in the clinical course might contribute to an understanding of brain function, as well as helping to design therapeutic interventions at the early stages of brain development.

We applied the ABA to a cohort of 13 CP patients and normal controls, age- and gender-paired. z-Score maps of the volume and FA values from two patients with very different image features were analyzed (Faria et al., 2011) (Fig. 6). The most evident characteristic of Patient #1 was the ventricle enlargement and the reduction of the white matter. Patient #2 images were marked by abnormal intensities in the white matter (hyper ADC and hypo FA areas) due to PVL, even though the patient also had large ventricles and a certain degree of white matter reduction. Focusing on the left superior longitudinal fasciculus (SLF, arrows), for example, visual inspection of the FA images of the patients reveals a smaller SLF, particularly in Patient #1, with possibly lower FA values, particularly in Patient #2. However, it is not straightforward to determine whether these maps are beyond the normal range of variability. For each segment, age-dependence and variability range was calculated from the control data, and deviations were delineated by z-scores, as shown in the leftmost column of Fig. 6. The actual fitting results for the left SLF are shown in the graphics. Our results indicate that the CP patients (yellow squares) had smaller FA and volumes than the average control values. Patients #1 and #2 had FA values lower than controls by more than four standard deviations, and volumes lower than controls by more than three standard deviations. Note that the SLF of Patient #2 showed even lower FA values, with a z-score near −10, while the SLF in Patient #1 had an even lower volume, with a z-score near −4, which is in agreement with our visual impression.

### 5.2. Williams syndrome

Williams syndrome (WS) is a genetic developmental disorder characterized by relatively strong language skills and severely impaired visuospatial abilities. Using T1-weighted images for volumetric analysis and DTI for diffusivity analysis, we observed that individuals with WS have atrophy in the basal ganglia and white matter (Fig. 7A and B), while the fusiform, medial temporal gyri, and the cerebellar cortex are relatively preserved (Fig. 7C) (Faria et al., 2012b). The DTI analysis indicated that the right superior longitudinal fasciculus, the left fronto-occipital fasciculus, the caudate, and the cingulum have increased FA, whereas the corticospinal tract shows decreased FA.

### 5.3. Rett syndrome

Rett syndrome (RS) is a neurological disorder, primarily affecting females, associated with global brain atrophy, more severe in the frontal, occipital, and dorsal parietal regions. However, the anatomical basis for this volumetric reduction, and the potential changes in diffusivity associated with this disease is uncertain. In a cohort of nine individuals with RS, we confirmed the previous results regarding brain atrophy. In addition, reduced FA was identified in the left peripheral white matter areas (the middle temporal, middle occipital,

pre-cuneus, and the post-central white matter), left major white matter tracts (the superior longitudinal fasciculus, sagittal stratum, corpus callosum), and the bilateral cingulum (Fig. 8).

### 5.4. Future directions: multimodal image analysis and personalization

Pediatric MRI studies, to date, have been primarily based on single-modality and on group comparisons. These strategies are useful for detecting anatomical features of diseased brains. The next logical step is to apply these findings to a single patient for an image-based diagnosis and clinical decision-making. Indeed, even when the pathology is clearly detected by group analysis, this type of analysis may not have enough statistical power for an individual-based diagnosis or decision-making.

A multimodal approach has been shown to classify various diseases more accurately than a single-modality approach (Allder et al., 2003; Brockmann et al., 2003; Kauczor, 2005; Rostasy et al., 2003; Wiest et al., 2005). Assuming that there are multiple pathologies with different spatial distributions in a single disease, the optimized combination of multiple MR modalities could increase the power to separate diseased brains from normal brains. One of the biggest challenges for multi-modal analysis is to establish a common anatomical framework that can integrate intra-subject as well as cross-subject multi-modal imaging data, which allows structure-by-structure, location-dependent statistical analysis. The ABA was applied to serve as the common anatomical framework (Faria et al., 2012a; Oishi et al., 2011c, 2009).

To appropriately combine information from multiple anatomical structures and multiple image modalities, various learning algorithms have been employed (Avants et al., 2010; Dukart et al., 2011; Franco et al., 2008; Hasan et al., 2012; Kloppel et al., 2008; Oishi et al., 2011a; Teipel et al., 2007; Zhang et al., 2011a). These methods are designed to provide appropriate weighting to each of the measured values of each structure. Fig. 9 is an attempt to integrate quantified volumes and DTI-derived intensities from several separate groups with different clinical categories and severities of CP. An unsupervised learning algorithm, principal component analysis (PCA), was applied to integrate multiple variables and to investigate the most influential axes that could effectively characterize the anatomical differences among groups (Yoshida et al., 2013a).

Once the multimodal data is combined, based on learning algorithms, the result can be personalized. For example, from training datasets that included groups of patients and control individuals, the vector that can most effectively separate the group with disease from the control group (diagnostic feature vector) could be generated. This diagnostic feature vector can be applied to an image from a new patient to calculate a projection, which can determine whether the patient should be categorized as having the disease.

## 6. Conclusion

An automated structure parcellation method, customized for neonatal and pediatric brain MRI, has been introduced, with the neonatal and pediatric brain atlases freely downloadable from our website (http://cmrm.med.jhmi.edu/ and www.MRIstudio.org). This method enables the quantification of multiple MR modalities using a common analytic framework. We attempted to create an MRI- and DTI-based growth percentile chart, followed by the application of that chart to investigate developmental abnormalities related to cerebral palsy, Williams syndrome, and Rett syndrome. Future directions include multimodal image analysis and personalization in the clinical settings.

## Acknowledgments

The authors thank Dr. Jon Skranes and Dr. Thomas Ernst for their helpful comments, and Ms. Mary McAllister for manuscript editing. This publication was made possible by grants from the National Institutes of Health (R21AG033774, R01HD065955, K24DA016170, R01MH061427, U54NS56883, P41RR015241, R03EB014357, RO1AG20012, and P50AG005146), and from the National Center for Research Resources grant G12-RR003061. Its contents are solely the responsibility of the authors and do not necessarily represent the official view of any of these Institutes.

## References

Cerebral Cortex. 2012; 22:1–12.

Aljabar P, Heckemann RA, Hammers A, Hajnal JV, Rueckert D. Multi-atlas based segmentation of brain images: atlas selection and its effect on accuracy. Neuroimage. 2009; 46:726–738. [PubMed: 19245840]

Allder SJ, Moody AR, Martel AL, Morgan PS, Delay GS, Gladman JR, Lennox GG. Differences in the diagnostic accuracy of acute stroke clinical subtypes defined by multimodal magnetic resonance imaging. Journal of Neurology, Neurosurgery and Psychiatry. 2003; 74:886–888.

Almli CR, Rivkin MJ, McKinstry RC. The NIH MRI study of normal brain development (Objective-2): newborns, infants, toddlers, and preschoolers. Neuroimage. 2007; 35:308–325. [PubMed: 17239623]

Arnould MC, Grandin CB, Peeters A, Cosnard G, Duprez TP. Comparison of CT and three MR sequences for detecting and categorizing early (48 h) hemorrhagic transformation in hyperacute ischemic stroke. AJNR – American Journal of Neuroradiology. 2004; 25:939–944. [PubMed: 15205127]

Artaechevarria X, Munoz-Barrutia A, Ortiz-de-Solorzano C. Combination strategies in multi-atlas image segmentation: application to brain MR data. IEEE Transactions on Medical Imaging. 2009; 28:1266–1277. [PubMed: 19228554]

Arzoumanian Y, Mirmiran M, Barnes PD, Woolley K, Ariagno RL, Moseley ME, Fleisher BE, Atlas SW. Diffusion tensor brain imaging findings at term-equivalent age may predict neurologic abnormalities in low birth weight preterm infants. AJNR – American Journal of Neuroradiology. 2003; 24:1646–1653. [PubMed: 13679287]

Avants BB, Cook PA, Ungar L, Gee JC, Grossman M. Dementia induces correlated reductions in white matter integrity and cortical thickness: a multivariate neuroimaging study with sparse canonical correlation analysis. Neuroimage. 2010; 50:1004–1016. [PubMed: 20083207]

Ball G, Counsell SJ, Anjari M, Merchant N, Arichi T, Doria V, Rutherford MA, Edwards AD, Rueckert D, Boardman JP. An optimised tract-based spatial statistics protocol for neonates: applications to prematurity and chronic lung disease. Neuroimage. 2010; 53:94–102. [PubMed: 20510375]

Bammer R, Markl M, Barnett A, Acar B, Alley MT, Pelc NJ, Glover GH, Moseley ME. Analysis and generalized correction of the effect of spatial gradient field distortions in diffusion-weighted imaging. Magnetic Resonance in Medicine. 2003; 50:560–569. [PubMed: 12939764]

Barkovich AJ, Kjos BO, Jackson DE Jr, Norman D. Normal maturation of the neonatal and infant brain: MR imaging at 1.5 T. Radiology. 1988; 166:173–180. [PubMed: 3336675]

Basser PJ, Mattiello J, LeBihan D. MR diffusion tensor spectroscopy and imaging. Biophysical Journal. 1994; 66:259–267. [PubMed: 8130344]

Beaulieu C, Allen PS. Determinants of anisotropic water diffusion in nerves. Magnetic Resonance in Medicine. 1994; 31:394–400. [PubMed: 8208115]

Beaulieu C, Fenrich FR, Allen PS. Multicomponent water proton transverse relaxation and T2-discriminated water diffusion in myelinated and nonmyelinated nerve. Magnetic Resonance Imaging. 1998; 16:1201–1210. [PubMed: 9858277]

Bennett CM, Baird AA. Anatomical changes in the emerging adult brain: a voxel-based morphometry study. Human Brain Mapping. 2006; 27:766–777. [PubMed: 16317714]

Berman JI, Mukherjee P, Partridge SC, Miller SP, Ferriero DM, Barkovich AJ, Vigneron DB, Henry RG. Quantitative diffusion tensor MRI fiber tractography of sensorimotor white matter development in premature infants. Neuroimage. 2005; 27:862–871. [PubMed: 15978841]

Boccardi M, Ganzola R, Bocchetta M, Pievani M, Redolfi A, Bartzokis G, Camicioli R, Csernansky JG, de Leon MJ, deToledo-Morrell L, Killiany RJ, Lehericy S, Pantel J, Pruessner JC, Soininen H, Watson C, Duchesne S, Jack CR Jr, Frisoni GB. Survey of protocols for the manual segmentation of the hippocampus: preparatory steps towards a joint EADC-ADNI harmonized protocol. Journal of Alzheimer's Disease. 2011; 26(Suppl. 3):61–75.

Brockmann K, Dechent P, Wilken B, Rusch O, Frahm J, Hanefeld F. Proton MRS profile of cerebral metabolic abnormalities in Krabbe disease. Neurology. 2003; 60:819–825. [PubMed: 12629240]

Cascio CJ, Gerig G, Piven J. Diffusion tensor imaging: Application to the study of the developing brain. Journal of the American Academy of Child & Adolescent Psychiatry. 2007; 46:213–223. [PubMed: 17242625]

Ceritoglu C, Oishi K, Li X, Chou MC, Younes L, Albert M, Lyketsos C, van Zijl PC, Miller MI, Mori S. Multi-contrast large deformation diffeomorphic metric mapping for diffusion tensor imaging. Neuroimage. 2009

Chang L, Smith LM, LoPresti C, Yonekura ML, Kuo J, Walot I, Ernst T. Smaller subcortical volumes and cognitive deficits in children with prenatal methamphetamine exposure. Psychiatry Research. 2004; 132:95–106. [PubMed: 15598544]

Chang LC, Jones DK, Pierpaoli C. RESTORE: robust estimation of tensors by outlier rejection. Magnetic Resonance in Medicine. 2005; 53:1088–1095. [PubMed: 15844157]

Clouchoux C, Limperopoulos C. Novel applications of quantitative MRI for the fetal brain. Pediatric Radiology. 2012; 42(Suppl 1):S24–S32. [PubMed: 22395718]

Collins DL, Holmes CJ, Peters TM, Evans AC. Automatic 3-D model-based neuroanatomical segmentation. Human Brain Mapping. 1995; 3:190–208.

Conturo TE, McKinstry RC, Akbudak E, Robinson BH. Encoding of anisotropic diffusion with tetrahedral gradients: a general mathematical diffusion formalism and experimental results. Magnetic Resonance in Medicine. 1996; 35:399–412. [PubMed: 8699953]

Davatzikos C. Why voxel-based morphometric analysis should be used with great caution when characterizing group differences. Neuroimage. 2004; 23:17–20. [PubMed: 15325347]

Ding XQ, Kucinski T, Wittkugel O, Goebell E, Grzyska U, Gorg M, Kohlschutter A, Zeumer H. Normal brain maturation characterized with age-related T2 relaxation times: an attempt to develop a quantitative imaging measure for clinical use. Investigative Radiology. 2004; 39:740–746. [PubMed: 15550835]

Ding XQ, Wittkugel O, Goebell E, Forster AF, Grzyska U, Zeumer H, Fiehler J. Clinical applications of quantitative T2 determination: a complementary MRI tool for routine diagnosis of suspected myelination disorders. European Journal of Paediatric Neurology. 2008; 12:298–308. [PubMed: 17964834]

Dubois J, Hertz-Pannier L, Dehaene-Lambertz G, Cointepas Y, Le Bihan D. Assessment of the early organization and maturation of infants' cerebral white matter fiber bundles: a feasibility study using quantitative diffusion tensor imaging and tractography. Neuroimage. 2006; 30:1121–1132. [PubMed: 16413790]

Dubois J, Dehaene-Lambertz G, Perrin M, Mangin JF, Cointepas Y, Duchesnay E, Le Bihan D, Hertz-Pannier L. Asynchrony of the early maturation of white matter bundles in healthy infants: quantitative landmarks revealed noninvasively by diffusion tensor imaging. Human Brain Mapping. 2008; 29:14–27. [PubMed: 17318834]

Dukart J, Mueller K, Horstmann A, Barthel H, Moller HE, Villringer A, Sabri O, Schroeter ML. Combined evaluation of FDG-PET and MRI improves detection and differentiation of dementia. PLoS ONE. 2011; 6:e18111. [PubMed: 21448435]

Dyakin VV, Chen Y, Branch CA, Veeranna Yuan A, Rao M, Kumar A, Peter-hoff CM, Nixon RA. The contributions of myelin and axonal caliber to transverse relaxation time in shiverer and neurofilament-deficient mouse models. Neuroimage. 2010; 51:1098–1105. [PubMed: 20226865]

Eikenes L, Lohaugen GC, Brubakk AM, Skranes J, Haberg AK. Young adults born preterm with very low birth weight demonstrate widespread white matter alterations on brain DTI. Neuroimage. 2011; 54:1774–1785. [PubMed: 20965255]

Evans AC. The NIH MRI study of normal brain development. Neuroimage. 2006; 30:184–202. [PubMed: 16376577]

Faria AV, Hoon A, Stashinko E, Li X, Jiang H, Mashayekh A, Akhter K, Hsu J, Oishi K, Zhang J, Miller MI, van Zijl PC, Mori S. Quantitative analysis of brain pathology based on MRI and brain atlases–applications for cerebral palsy. Neuroimage. 2011; 54:1854–1861. [PubMed: 20920589]

Faria AV, Joel SE, Zhang Y, Oishi K, van Zjil PC, Miller MI, Pekar JJ, Mori S. Atlas-based analysis of resting-state functional connectivity: evaluation for reproducibility and multi-modal anatomy–function correlation studies. Neuroimage. 2012a

Faria AV, Landau B, O'Hearn KM, Li X, Jiang H, Oishi K, Zhang J, Mori S. Quantitative analysis of gray and white matter in Williams syndrome. Neuroreport. 2012b; 23:283–289. [PubMed: 22410548]

Faria AV, Zhang J, Oishi K, Li X, Jiang H, Akhter K, Hermoye L, Lee SK, Hoon A, Stashinko E, Miller MI, van Zijl PC, Mori S. Atlas-based analysis of neurodevelopment from infancy to adulthood using diffusion tensor imaging and applications for automated abnormality detection. Neuroimage. 2010; 52:415–428. [PubMed: 20420929]

Farrell JA, Landman BA, Jones CK, Smith SA, Prince JL, van Zijl PC, Mori S. Effects of signal-to-noise ratio on the accuracy and reproducibility of diffusion tensor imaging-derived fractional anisotropy, mean diffusivity, and principal eigenvector measurements at 1.5 T. Journal of Magnetic Resonance Imaging. 2007; 26:756–767. [PubMed: 17729339]

Ferrie JC, Barantin L, Saliba E, Akoka S, Tranquart F, Sirinelli D, Pourcelot L. MR assessment of the brain maturation during the perinatal period: quantitative T2 MR study in premature newborns. Magnetic Resonance Imaging. 1999; 17:1275–1288. [PubMed: 10576713]

Fischl B, Salat DH, Busa E, Albert M, Dieterich M, Haselgrove C, van der Kouwe A, Killiany R, Kennedy D, Klaveness S, Montillo A, Makris N, Rosen B, Dale AM. Whole brain segmentation: automated labeling of neuroanatomical structures in the human brain. Neuron. 2002; 33:341–355. [PubMed: 11832223]

Franco AR, Ling J, Caprihan A, Calhoun VD, Jung RE, Heileman GL, Mayer AR. Multimodal and multi-tissue measures of connectivity revealed by joint independent component analysis. IEEE Journal of Selected Topics in Signal Processing. 2008; 2:986–997. [PubMed: 19777078]

Gao W, Lin W, Chen Y, Gerig G, Smith JK, Jewells V, Gilmore JH. Temporal and spatial development of axonal maturation and myelination of white matter in the developing brain. American Journal of Neuroradiology. 2009; 30:290–296. [PubMed: 19001533]

Giedd JN, Blumenthal J, Jeffries NO, Castellanos FX, Liu H, Zijdenbos A, Paus T, Evans AC, Rapoport JL. Brain development during childhood and adolescence: a longitudinal MRI study. Nature Neuroscience. 1999; 2:861–863.

Gilmore JH, Lin W, Corouge I, Vetsa YS, Smith JK, Kang C, Gu H, Hamer RM, Lieberman JA, Gerig G. Early postnatal development of corpus callosum and corticospinal white matter assessed with quantitative tractography. AJNR – American Journal of Neuroradiology. 2007; 28:1789–1795. [PubMed: 17923457]

Gimenez M, Junque C, Narberhaus A, Bargallo N, Botet F, Mercader JM. White matter volume and concentration reductions in adolescents with history of very preterm birth: a voxel-based morphometry study. Neuroimage. 2006; 32:1485–1498. [PubMed: 16809052]

Gimenez M, Miranda MJ, Born AP, Nagy Z, Rostrup E, Jernigan TL. Accelerated cerebral white matter development in preterm infants: a voxel-based morphometry study with diffusion tensor MR imaging. Neuroimage. 2008; 41:728–734. [PubMed: 18430590]

Hasan KM, Walimuni IS, Abid H, Datta S, Wolinsky JS, Narayana PA. Human brain atlas-based multimodal MRI analysis of volumetry, diffusimetry, relaxometry and lesion distribution in multiple sclerosis patients and healthy adult controls: implications for understanding the pathogenesis of multiple sclerosis and consolidation of quantitative MRI results in MS. Journal of the Neurological Sciences. 2012; 313:99–109. [PubMed: 21978603]

Heckemann RA, Hajnal JV, Aljabar P, Rueckert D, Hammers A. Automatic anatomical brain MRI segmentation combining label propagation and decision fusion. Neuroimage. 2006; 33:115–126. [PubMed: 16860573]

Heckemann RA, Keihaninejad S, Aljabar P, Rueckert D, Hajnal JV, Hammers A. Improving intersubject image registration using tissue-class information benefits robustness and accuracy of multi-atlas based anatomical segmentation. Neuroimage. 2010; 51:221–227. [PubMed: 20114079]

Hermoye L, Saint-Martin C, Cosnard G, Lee SK, Kim J, Nassogne MC, Menten R, Clapuyt P, Donohue PK, Hua K, Wakana S, Jiang H, van Zijl PC, Mori S. Pediatric diffusion tensor imaging: normal database and observation of the white matter maturation in early childhood. Neuroimage. 2006; 29:493–504. [PubMed: 16194615]

Hsu EW, Mori S. Analytical expressions for the NMR apparent diffusion coefficients in an anisotropic system and a simplified method for determining fiber orientation. Magnetic Resonance in Medicine. 1995; 34:194–200. [PubMed: 7476078]

Huang H, Zhang J, Wakana S, Zhang W, Ren T, Richards LJ, Yarowsky P, Donohue P, Graham E, van Zijl PC, Mori S. White and gray matter development in human fetal, newborn and pediatric brains. Neuroimage. 2006; 33:27–38. [PubMed: 16905335]

Huppi PS, Warfield S, Kikinis R, Barnes PD, Zientara GP, Jolesz FA, Tsuji MK, Volpe JJ. Quantitative magnetic resonance imaging of brain development in premature and mature newborns. Annals of Neurology. 1998; 43:224–235. [PubMed: 9485064]

Inder TE, Anderson NJ, Spencer C, Wells S, Volpe JJ. White matter injury in the premature infant: a comparison between serial cranial sonographic and MR findings at term. AJNR – American Journal of Neuroradiology. 2003; 24:805–809. [PubMed: 12748075]

Jack CR Jr, O'Brien PC, Rettman DW, Shiung MM, Xu Y, Muthupillai R, Manduca A, Avula R, Erickson BJ. FLAIR histogram segmentation for measurement of leukoaraiosis volume. Journal of Magnetic Resonance Imaging. 2001; 14:668–676. [PubMed: 11747022]

Jacob FD, Habas PA, Kim K, Corbett-Detig J, Xu D, Studholme C, Glenn OA. Fetal hippocampal development: analysis by magnetic resonance imaging volumetry. Pediatric Research. 2011; 69:425–429. [PubMed: 21270675]

Jia H, Yap PT, Shen D. Iterative multi-atlas-based multi-image segmentation with tree-based registration. Neuroimage. 2012; 59:422–430. [PubMed: 21807102]

Jiang H, van Zijl PC, Kim J, Pearlson GD, Mori S. DtiStudio: resource program for diffusion tensor computation and fiber bundle tracking. Computer Methods and Programs in Biomedicine. 2006; 81:106–116. [PubMed: 16413083]

Jones DK, Basser PJ. Squashing peanuts and smashing pumpkins: how noise distorts diffusion-weighted MR data. Magnetic Resonance in Medicine. 2004; 52:979–993. [PubMed: 15508154]

Joshi S, Davis B, Jomier M, Gerig G. Unbiased diffeomorphic atlas construction for computational anatomy. Neuroimage. 2004; 23(Suppl. 1):S151L 160. [PubMed: 15501084]

Kauczor HU. Multimodal imaging and computer assisted diagnosis for functional tumour characterisation. Cancer Imaging. 2005; 5:46–50. [PubMed: 16154819]

Kinney HC, Brody BA, Kloman AS, Gilles FH. Sequence of central nervous system myelination in human infancy. II. Patterns of myelination in autopsied infants. Journal of Neuropathology and Experimental Neurology. 1988; 47:217–234. [PubMed: 3367155]

Klein A, Hirsch J. Mindboggle: a scatterbrained approach to automate brain labeling. Neuroimage. 2005; 24:261–280. [PubMed: 15627570]

Kloppel S, Stonnington CM, Chu C, Draganski B, Scahill RI, Rohrer JD, Fox NC, Jack CR Jr, Ashburner J, Frackowiak RS. Automatic classification of MR scans in Alzheimer's disease. Brain. 2008; 131:681–689. [PubMed: 18202106]

Koay CG, Chang LC, Carew JD, Pierpaoli C, Basser PJ. A unifying theoretical and algorithmic framework for least squares methods of estimation in diffusion tensor imaging. Journal of Magnetic Resonance. 2006; 182:115–125. [PubMed: 16828568]

Landman BA, Farrell JA, Jones CK, Smith SA, Prince JL, Mori S. Effects of diffusion weighting schemes on the reproducibility of DTI-derived fractional anisotropy, mean diffusivity, and principal eigenvector measurements at 1.5 T. Neuroimage. 2007; 36:1123–1138. [PubMed: 17532649]

Langerak TR, van der Heide UA, Kotte AN, Viergever MA, van Vulpen M, Pluim JP. Label fusion in atlas-based segmentation using a selective and iterative method for performance level estimation (SIMPLE). IEEE Transactions on Medical Imaging. 2010; 29:2000–2008. [PubMed: 20667809]

Li, Y.; Shea, SM.; Jiang, H.; Lorenz, CH.; Mori, S. International Conference for Magnetic Resonance in Medicine. Stockholm, Sweden: 2010. Improved, real-time artifact detection and reacquisiton for diffusion tensor imaging (DTI).

Lindqvist S, Skranes J, Eikenes L, Haraldseth O, Vik T, Brubakk AM, Vangberg TR. Visual function and white matter microstructure in very-low-birth-weight (VLBW) adolescents—a DTI study. Vision Research. 2011; 51:2063–2070. [PubMed: 21854799]

Lobel U, Sedlacik J, Gullmar D, Kaiser WA, Reichenbach JR, Mentzel HJ. Diffusion tensor imaging: the normal evolution of ADC, RA, FA, and eigenvalues studied in multiple anatomical regions of the brain. Neuroradiology. 2009; 51:253–263. [PubMed: 19132355]

Lodygensky GA, Seghier ML, Warfield SK, Tolsa CB, Sizonenko S, Lazeyras F, Huppi PS. Intrauterine growth restriction affects the preterm infant's hippocampus. Pediatric Research. 2008; 63:438–443. [PubMed: 18356754]

Maldjian JA, Laurienti PJ, Kraft RA, Burdette JH. An automated method for neuroanatomic and cytoarchitectonic atlas-based interrogation of fMRI data sets. Neuroimage. 2003; 19:1233–1239. [PubMed: 12880848]

Mallar Chakravarty M, Steadman P, van Eede MC, Calcott RD, Gu V, Shaw P, Raznahan A, Louis Collins D, Lerch JP. Performing label-fusion-based segmentation using multiple automatically generated templates. Human Brain Mapping. 2012

Mathur AM, Neil JJ, Inder TE. Understanding brain injury and neurode-velopmental disabilities in the preterm infant: the evolving role of advanced magnetic resonance imaging. Seminars in Perinatology. 2010; 34:57–66. [PubMed: 20109973]

McKinstry RC, Mathur A, Miller JH, Ozcan A, Snyder AZ, Schefft GL, Almli CR, Shiran SI, Conturo TE, Neil JJ. Radial organization of developing preterm human cerebral cortex revealed by non-invasive water diffusion anisotropy MRI. Cerebral Cortex. 2002; 12:1237–1243. [PubMed: 12427675]

Ment LR, Hirtz D, Huppi PS. Imaging biomarkers of outcome in the developing preterm brain. The Lancet Neurology. 2009; 8:1042–1055.

Miller SP, Vigneron DB, Henry RG, Bohland MA, Ceppi-Cozzio C, Hoffman C, Newton N, Partridge JC, Ferriero DM, Barkovich AJ. Serial quantitative diffusion tensor MRI of the premature brain: development in newborns with and without injury. Journal of Magnetic Resonance Imaging. 2002; 16:621–632. [PubMed: 12451575]

Miot-Noirault E, Barantin L, Akoka S, Le Pape A. T2 relaxation time as a marker of brain myelination: experimental MR study in two neonatal animal models. Journal of Neuroscience Methods. 1997; 72:5–14. [PubMed: 9128162]

Miot E, Hoffschir D, Poncy JL, Masse R, Le Pape A, Akoka S. Magnetic resonance imaging in vivo monitoring of T2 relaxation time: quantitative assessment of primate brain maturation. Journal of Medical Primatology. 1995; 24:87–93. [PubMed: 8613978]

Mori S, Itoh R, Zhang J, Kaufmann WE, van Zijl PC, Solaiyappan M, Yarowsky P. Diffusion tensor imaging of the developing mouse brain. Magnetic Resonance in Medicine. 2001; 46:18–23. [PubMed: 11443706]

Mori S, Oishi K, Faria AV, Miller MI. Atlas-based neuroinformatics via MRI: harnessing the information from past clinical cases and quantitative image analysis for patient care. Annual Review of Biomedical Engineering. 2013

Mori S, Oishi K, Jiang H, Jiang L, Li X, Akhter K, Hua K, Faria AV, Mahmood A, Woods R, Toga AW, Pike GB, Neto PR, Evans A, Zhang J, Huang H, Miller MI, van Zijl P, Mazziotta J. Stereotaxic white matter atlas based on diffusion tensor imaging in an ICBM template. Neuroimage. 2008; 40:570–582. [PubMed: 18255316]

Mukherjee P, Miller JH, Shimony JS, Philip JV, Nehra D, Snyder AZ, Conturo TE, Neil JJ, McKinstry RC. Diffusion-tensor MR imaging of gray and white matter development during normal human brain maturation. AJNR - American Journal of Neuroradiology. 2002; 23:1445–1456. [PubMed: 12372731]

Muzik O, Chugani DC, Juhasz C, Shen C, Chugani HT. Statistical parametric mapping: assessment of application in children. Neuroimage. 2000; 12:538–549. [PubMed: 11034861]

Neil JJ, Shiran SI, McKinstry RC, Schefft GL, Snyder AZ, Almli CR, Akbudak E, Aronovitz JA, Miller JP, Lee BC, Conturo TE. Normal brain in human newborns: apparent diffusion coefficient and diffusion anisotropy measured by using diffusion tensor MR imaging. Radiology. 1998; 209:57–66. [PubMed: 9769812]

Oishi K, Akhter K, Mielke M, Ceritoglu C, Zhang J, Jiang H, Li X, Younes L, Miller MI, van Zijl PC, Albert M, Lyketsos CG, Mori S. Multi-modal MRI analysis with disease-specific spatial filtering: initial testing to predict mild cognitive impairment patients who convert to Alzheimer's disease. Frontiers in Neurology. 2011a; 2:54. [PubMed: 21904533]

Oishi K, Faria A, Jiang H, Li X, Akhter K, Zhang J, Hsu JT, Miller MI, van Zijl PC, Albert M, Lyketsos CG, Woods R, Toga AW, Pike GB, Rosa-Neto P, Evans A, Mazziotta J, Mori S. Atlas-based whole brain white matter analysis using large deformation diffeomorphic metric mapping: application to normal elderly and Alzheimer's disease participantstlas. Neuroimage. 2009; 46:486–499. [PubMed: 19385016]

Oishi, K.; Faria, AV.; Mori, S., editors. Advanced Neonatal NeuroMRI. Elsevier, Amsterdum; 2012. 2011/11/29 ed.

Oishi K, Mielke MM, Albert M, Lyketsos CG, Mori S. DTI Analyses and Clinical Applications in Alzheimer's Disease. Handbook of Alzheimer's Disease IOS Press, Amsterdam, The Netherlands. 2011b

Oishi K, Mori S, Donohue P, Ernst TLA, Buchthal S, Faria A, Jiang H, Li XMIM, van Zijl P, Chang L. Multi-contrast human neonatal brain atlas: application to normal neonate development analysis. Neuroimage. 2011c; 56:8–20. [PubMed: 21276861]

Oishi K, Zilles K, Amunts K, Faria A, Jiang H, Li X, Akhter K, Hua K, Woods R, Toga AW, Pike GB, Rosa-Neto P, Evans A, Zhang J, Huang H, Miller MI, van Zijl PC, Mazziotta J, Mori S. Human brain white matteratlas: identification and assignment of common anatomical structures in superficial white matter. Neuroimage. 2008; 43:447–457. [PubMed: 18692144]

Pearce MS, Salotti JA, Little MP, McHugh K, Lee C, Kim KP, Howe NL, Ronck-ers CM, Rajaraman P, Craft AW, Parker L, de Gonzalez AB. Radiation exposure from CT scans in childhood and subsequent risk of leukaemia and brain tumours: a retrospective cohort study. Lancet. 2012

Pierpaoli C, Basser PJ. Toward a quantitative assessment of diffusion anisotropy. Magnetic Resonance in Medicine. 1996; 36:893–906. [PubMed: 8946355]

Pierpaoli C, Jezzard P, Basser PJ, Barnett A, Di Chiro G. Diffusion tensor MR imaging of the human brain. Radiology. 1996; 201:637–648. [PubMed: 8939209]

Rose J, Butler EE, Lamont LE, Barnes PD, Atlas SW, Stevenson DK. Neonatal brain structure on MRI and diffusion tensor imaging, sex, andneurode-velopment in very-low-birthweight preterm children. Developmental Medicine and Child Neurology. 2009; 51:526–535. [PubMed: 19459915]

Rostasy KM, Diepold K, Buckard J, Brockmann K, Wilken B, Hanefeld F. Progressive muscle weakness after high-dose steroids in two children with CIDP. Pediatric Neurology. 2003; 29:236–238. [PubMed: 14629908]

Rousseau F, Habas PA, Studholme C. A supervised patch-based approach for human brain labeling. IEEE Transactions on Medical Imaging. 2011; 30:1852–1862. [PubMed: 21606021]

Shaw P, Kabani NJ, Lerch JP, Eckstrand K, Lenroot R, Gogtay N, Greenstein D, Clasen L, Evans A, Rapoport JL, Giedd JN, Wise SP. Neurodevel-opmental trajectories of the human cerebral cortex. Journal of Neuroscience. 2008; 28:3586–3594. [PubMed: 18385317]

Shi F, Fan Y, Tang S, Gilmore JH, Lin W, Shen D. Neonatal brain image segmentation in longitudinal MRI studies. Neuroimage. 2009

Shi F, Yap PT, Fan Y, Gilmore JH, Lin W, Shen D. Construction of multi-region-multi-reference atlases for neonatal brain MRI segmentation. Neuroimage. 2010

Silk TJ, Wood AG. Lessons about neurodevelopment from anatomical magnetic resonance imaging. Journal of Developmental and Behavioral Pediatrics. 2011; 32:158–168. [PubMed: 21200332]

Skranes J, Lohaugen GC, Martinussen M, Indredavik MS, Dale AM, Haraldseth O, Vangberg TR, Brubakk AM. White matter abnormalities and executive function in children with very low birth weight. Neuroreport. 2009; 20:263–266. [PubMed: 19444947]

Skranes J, Vangberg TR, Kulseng S, Indredavik MS, Evensen KA, Martinussen M, Dale AM, Haraldseth O, Brubakk AM. Clinical findings and white matter abnormalities seen on diffusion tensor imaging in adolescents with very low birth weight. Brain. 2007; 130:654–666. [PubMed: 17347255]

Smith SM, Jenkinson M, Johansen-Berg H, Rueckert D, Nichols TE, Mackay CE, Watkins KE, Ciccarelli O, Cader MZ, Matthews PM, Behrens TE. Tract-based spatial statistics: voxelwise analysis of multi-subject diffusion data. Neuroimage. 2006; 31:1487–1505. [PubMed: 16624579]

Soria-Pastor S, Padilla N, Zubiaurre-Elorza L, Ibarretxe-Bilbao N, Botet F, Costas-Moragas C, Falcon C, Bargallo N, Mercader JM, Junque C. Decreased regional brain volume and cognitive impairment in preterm children at low risk. Pediatrics. 2009; 124:e1161–e1170. [PubMed: 19948618]

Studholme C. Dense feature deformation morphometry: incorporating DTI data into conventional MRI morphometry. Medical Image Analysis. 2008; 12:742–751. [PubMed: 18555734]

Talairach J, Tournoux P. Co-planar stereotaxic atlas of the human brain: 3-dimensional proportional system: an approach to cerebral imaging. Thieme. 1988

Tang X, Oishi K, Faria AV, Hillis AE, Albert MS, Mori S, Miller MI. Bayesian parameter estimation and segmentation in the multi-atlas random orbit model. PLoS ONE. 2013; 8:e65591. [PubMed: 23824159]

Teipel SJ, Stahl R, Dietrich O, Schoenberg SO, Perneczky R, Bokde AL, Reiser MF, Moller HJ, Hampel H. Multivariate network analysis of fiber tract integrity in Alzheimer's disease. Neuroimage. 2007; 34:985–995. [PubMed: 17166745]

Tzourio-Mazoyer N, Landeau B, Papathanassiou D, Crivello F, Etard O, Delcroix N, Mazoyer B, Joliot M. Automated anatomical labeling of activations in SPM using a macroscopic anatomical parcellation of the MNIMRI single-subject brain. Neuroimage. 2002; 15:273–289. [PubMed: 11771995]

Ueda T, Kanda F, Aoyama N, Fujii M, Nishigori C, Toda T. Neuroimaging features of xeroderma pigmentosum group A. Brain and Behavior. 2012; 2:1–5. [PubMed: 22574268]

Ulug AM, van Zijl PC. Orientation-independent diffusion imaging without tensor diagonalization: anisotropy definitions based on physical attributes of the diffusion ellipsoid. Journal of Magnetic Resonance Imaging. 1999; 9:804–813. [PubMed: 10373028]

van der Knaap MS, Valk J. MR imaging of the various stages of normal myelination during the first year of life. Neuroradiology. 1990; 31:459–470. [PubMed: 2352626]

van Rikxoort EM, Isgum I, Arzhaeva Y, Staring M, Klein S, Viergever MA, Pluim JP, van Ginneken B. Adaptive local multi-atlas segmentation: application to the heart and the caudate nucleus. Medical Image Analysis. 2010; 14:39–49. [PubMed: 19897403]

van Wezel-Meijler G, De Bruine FT, Steggerda SJ, Van den Berg-Huysmans A, Zeilemaker S, Leijser LM, Van der Grond J. Ultrasound detection of white matter injury in very preterm neonates: practical implications. Developmental Medicine and Child Neurology. 2011; 53(Suppl. 4):29–34. [PubMed: 21950391]

Vangberg TR, Skranes J, Dale AM, Martinussen M, Brubakk AM, Haraldseth O. Changes in white matter diffusion anisotropy in adolescents born prematurely. Neuroimage. 2006; 32:1538–1548. [PubMed: 16843682]

Waber DP, De Moor C, Forbes PW, Almli CR, Botteron KN, Leonard G, Milovan D, Paus T, Rumsey J. The NIH MRI study of normal brain development: performance of a population based sample of healthy children aged 6–18 years on a neuropsychological battery. Journal of the International Neuropsychological Society. 2007; 13:729–746. [PubMed: 17511896]

Warfield SK, Zou KH, Wells WM. Simultaneous truth and performance level estimation (STAPLE): an algorithm for the validation of image segmentation. IEEE Transactions on Medical Imaging. 2004; 23:903–921. [PubMed: 15250643]

Wiest R, Kassubek J, Schindler K, Loher TJ, Kiefer C, Mariani L, Wissmeyer M, Schroth G, Mathis J, Weder B, Juengling FD. Comparison of voxel-based 3-D MRI analysis and subtraction ictal SPECT coregistered to MRI in focal epilepsy. Epilepsy Research. 2005; 65:125–133. [PubMed: 15998582]

Wiggins RC. Myelination: a critical stage in development. Neurotoxicology. 1986; 7:103–120. [PubMed: 3537850]

Wilke M, Holland SK. Variability of gray and white matter during normal development: a voxel-based MRI analysis. Neuroreport. 2003; 14:1887–1890. [PubMed: 14561914]

Wilke M, Holland SK, Altaye M, Gaser C. Template-O-Matic: a toolbox for creating customized pediatric templates. Neuroimage. 2008; 41:903–913. [PubMed: 18424084]

Wilke M, Schmithorst VJ, Holland SK. Assessment of spatial normalization of whole-brain magnetic resonance images in children. Human Brain Mapping. 2002; 17:48–60. [PubMed: 12203688]

Wilke M, Schmithorst VJ, Holland SK. Normative pediatric brain data for spatial normalization and segmentation differs from standard adult data. Magnetic Resonance in Medicine. 2003; 50:749–757. [PubMed: 14523961]

Wu M, Rosano C, Lopez-Garcia P, Carter CS, Aizenstein HJ. Optimum template selection for atlas-based segmentation. Neuroimage. 2007; 34:1612–1618. [PubMed: 17188896]

Yakovlev, PI.; Lecours, AR. Regional Development of the Brain in Early Life. Philadelphia, PA: F.A. Davis; 1967.

Yoshida S, Faria A, Oishi K, Kanda T, Yamori Y, Yoshida N, Hirota H, Iwami M, Okano S, Hsu K, Jiang H, Li Y, Hayakawa K, Mori S. Anatomical characterization of athetotic and spastic cerebral palsy using an atlas-based analysis. Journal of Magnetic Resonance Imaging [in print]. 2013a

Yoshida S, Oishi K, Faria A, Mori S. Diffusion tensor imaging of normal brain development. Pediatric Radiology. 2013b; 43:3. [PubMed: 23229343]

Yushkevich PA, Avants BB, Pluta J, Das S, Minkoff D, Mechanic-Hamilton D, Glynn S, Pickup S, Liu W, Gee JC, Grossman M, Detre JA. A high-resolution computational atlas of the human hippocampus from postmortem magnetic resonance imaging at 9.4 T. Neuroimage. 2009; 44:385–398. [PubMed: 18840532]

Zhang D, Wang Y, Zhou L, Yuan H, Shen D. Multimodal classification of Alzheimer's disease and mild cognitive impairment. Neuroimage. 2011a; 55:856–867. [PubMed: 21236349]

Zhang J, Evans A, Hermoye L, Lee SK, Wakana S, Zhang W, Donohue P, Miller MI, Huang H, Wang X, van Zijl PC, Mori S. Evidence of slow maturation of the superior longitudinal fasciculus in early childhood by diffusion tensor imaging. Neuroimage. 2007; 38:239–247. [PubMed: 17826183]

Zhang Y, Zhang J, Ma J, Oishi K, Faria A, Miller M, Mori S. Creation of a population-representative brain atlas with clear anatomical definition. International Society for Magnetic Resonance in Medicine, Montreal, Canada. 2011b

Zhu T, Hu R, Qiu X, Taylor M, Tso Y, Yiannoutsos C, Navia B, Mori S, Ekholm S, Schifitto G, Zhong J. Quantification of accuracy and precision of multi-center DTI measurements: a diffusion phantom and human brain study. Neuroimage. 2011; 56:1398–1411. [PubMed: 21316471]

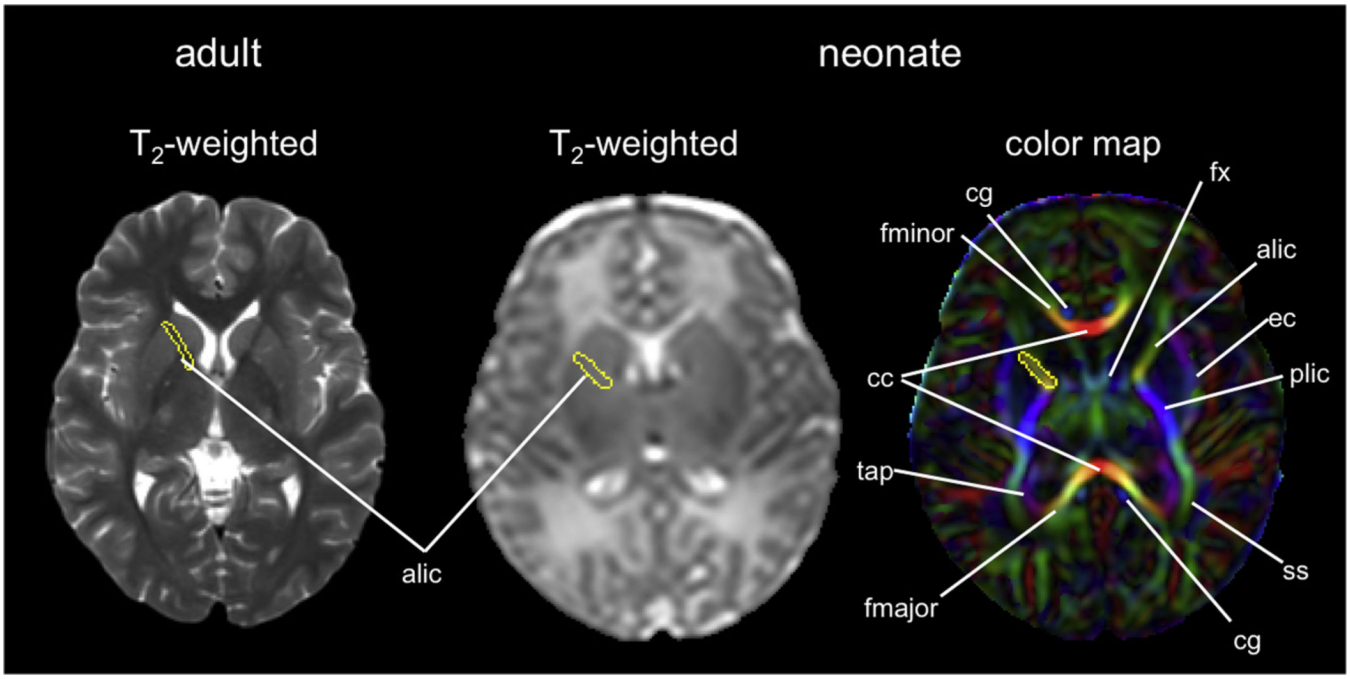


**Fig. 1.**

An example of an adult T2-weighted image and a neonatal (0 weeks old) T2-weighted image and color map. The anterior limb of the internal capsule is identified in the adult T2-weighted image, but is difficult to identify in the neonatal T2-weighted image. Using a color map, various white matter structures can be readily identified, even in the poorly myelinated neonatal brain. Coordinates of the anterior limb of the internal capsule were transferred from the color map to the T2-weighted image. alic/plic, anterior and posterior limb of internal capsule; cc, corpus callosum; cg, cingulum; ec, external capsule; fmajor/fminor, forceps major and minor; fx, fornix; ss, sagittal striatum; tap, tapatum.

From Oishi et al. (2012) with permission.

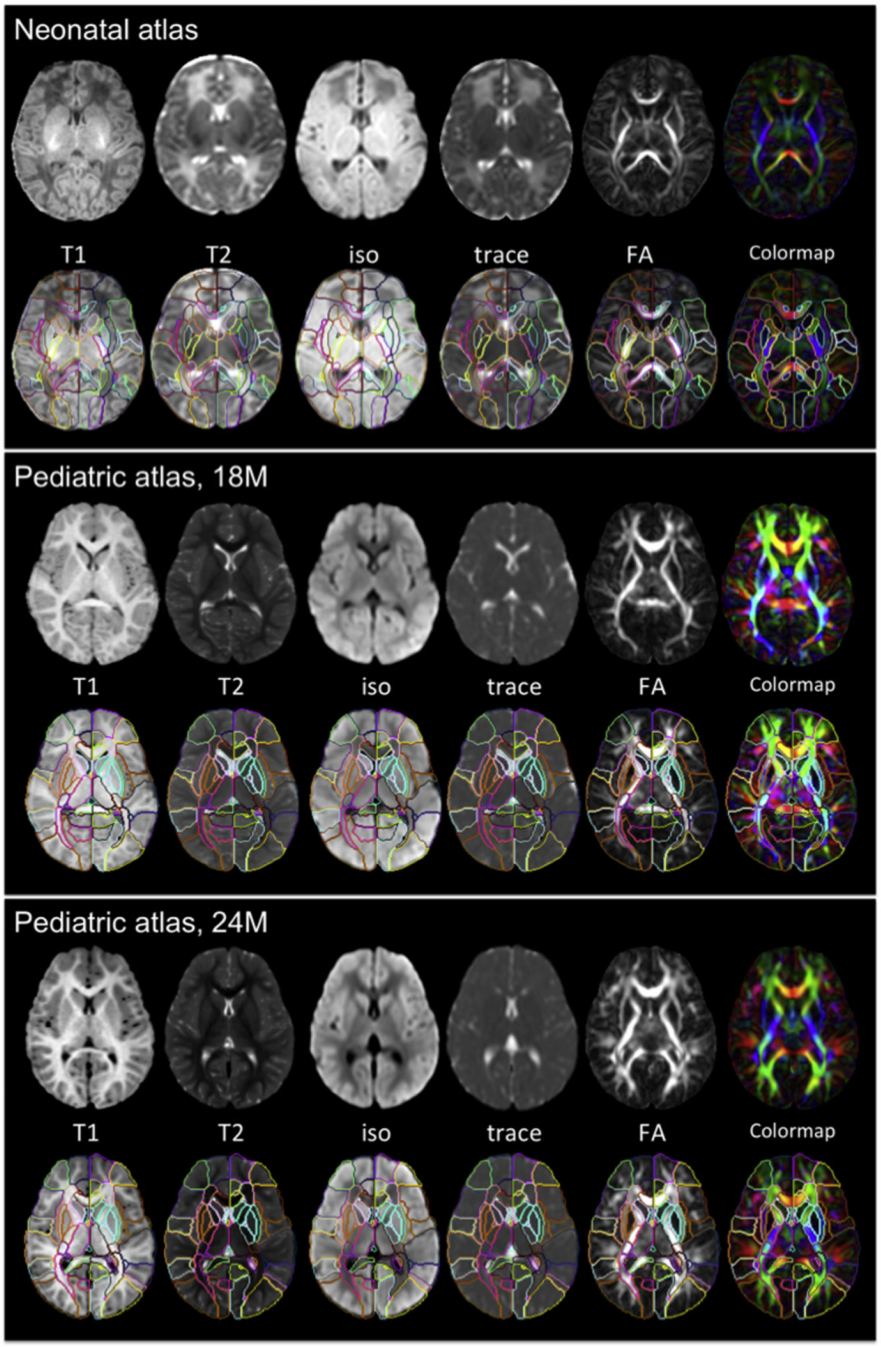


**Fig. 2.**

Multi-contrast, single-subject atlases for a neonate (with 112 parcellations) at two years old, 18 months old, and in an adult (with 159 parcellations) (available at http://lbam.med.jhmi.edu/).

From Oishi et al. (2011c) and Yoshida et al. (2013b) with permission.

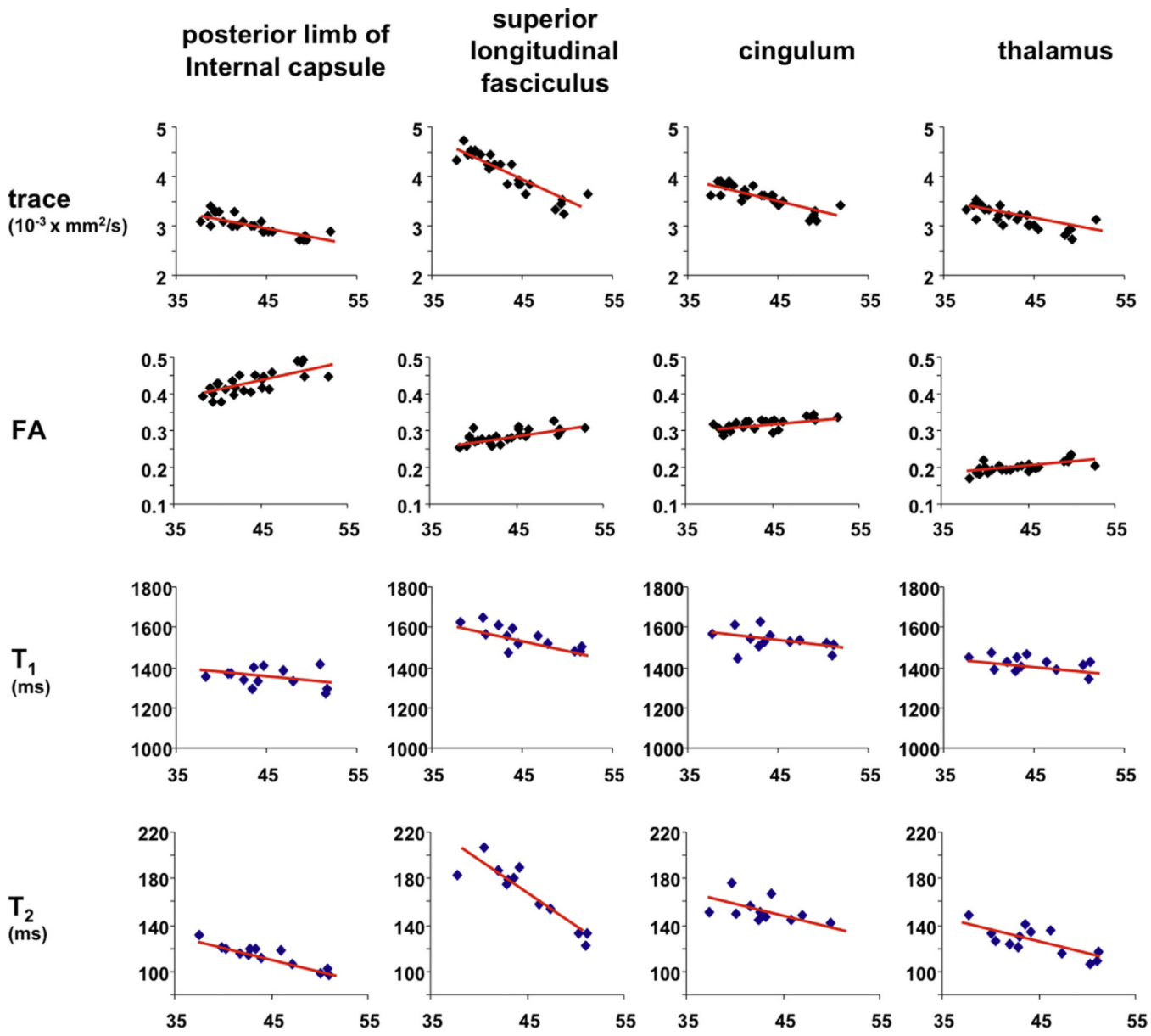


**Fig. 3.**

Representative scattergrams from the atlas-based image quantification showing the developmental pattern of each anatomical structure. The horizontal axis indicates post-menstrual weeks. The first row shows the age-dependent decreases in mean diffusivity (Trace) of each structure. The second row shows the age-dependent increases in FA. The third row shows the age-dependent decreases in T1, and the lowest row shows the age-dependent decreases in T2. The MR measures of each structure changed at different rates.

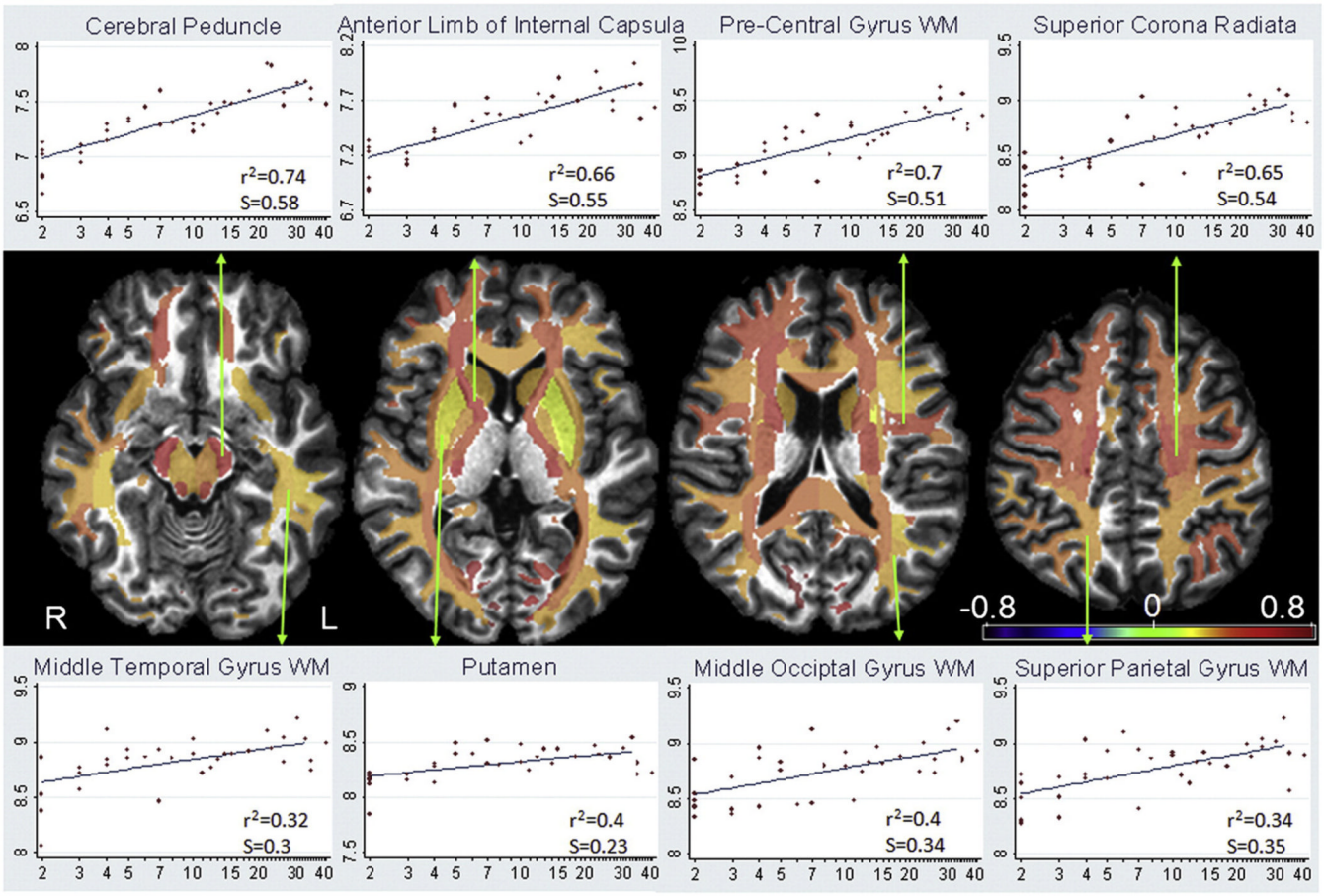


**Fig. 4.**

Examples of actual data points and the fitting results of the ABA at representative areas with high (upper row) and low (bottom row) volumetric age (year)-dependency. Note that the slopes were color-coded and mapped on the T1-atlas for visualization purposes, but the actual volume measurement was performed in original DTI space.

From Faria et al. (2010) with permission.

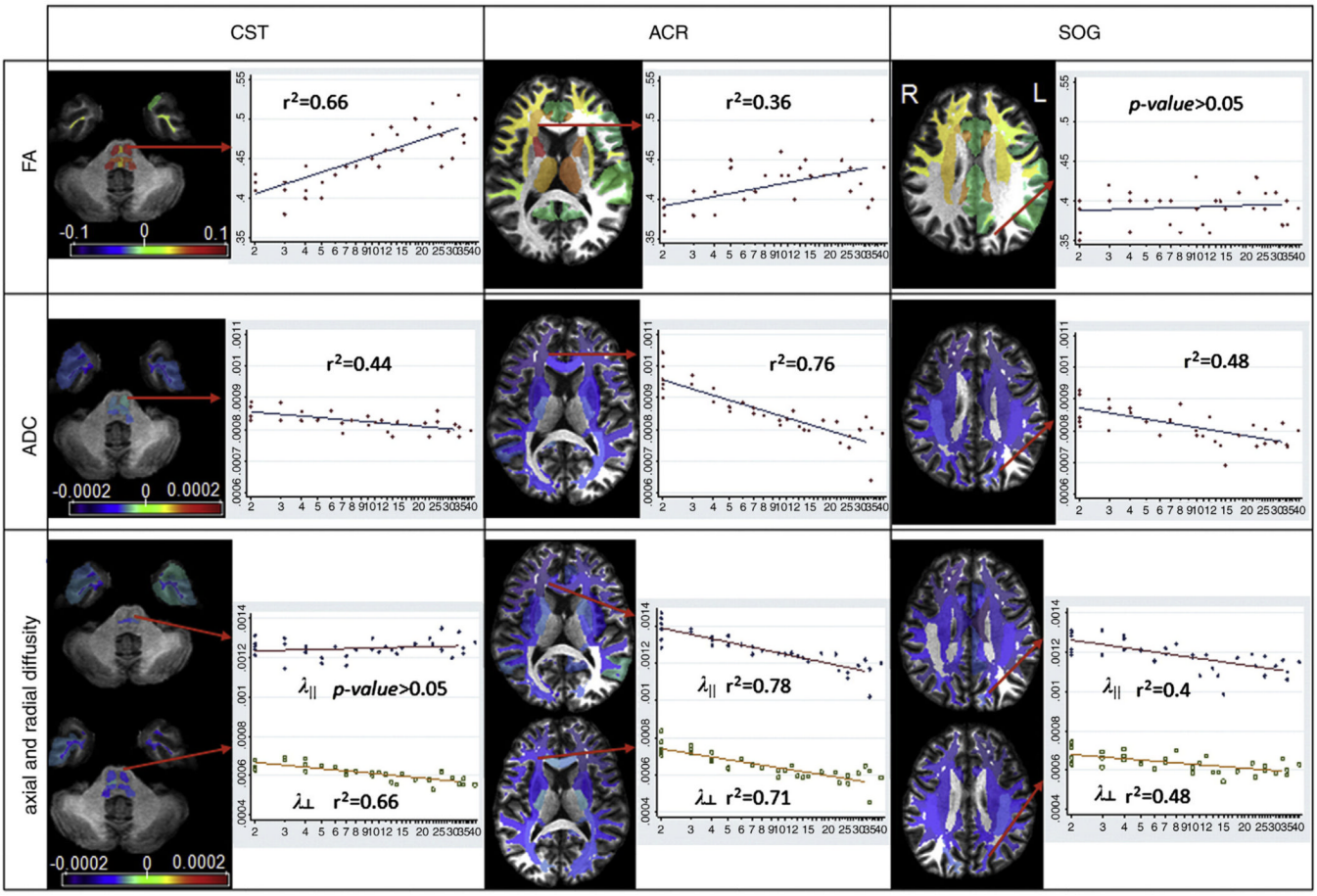


**Fig. 5.**

Three brain regions with different characteristics for age-dependent changes. These areas have high, low, and no significant age-dependency for FA, while all areas have a clear and significant ADC decline. CST, corticospinal tract; ACR, anterior corona radiata; SOG, white matter of the superior occipital gyrus.

From Faria et al. (2010) with permission.

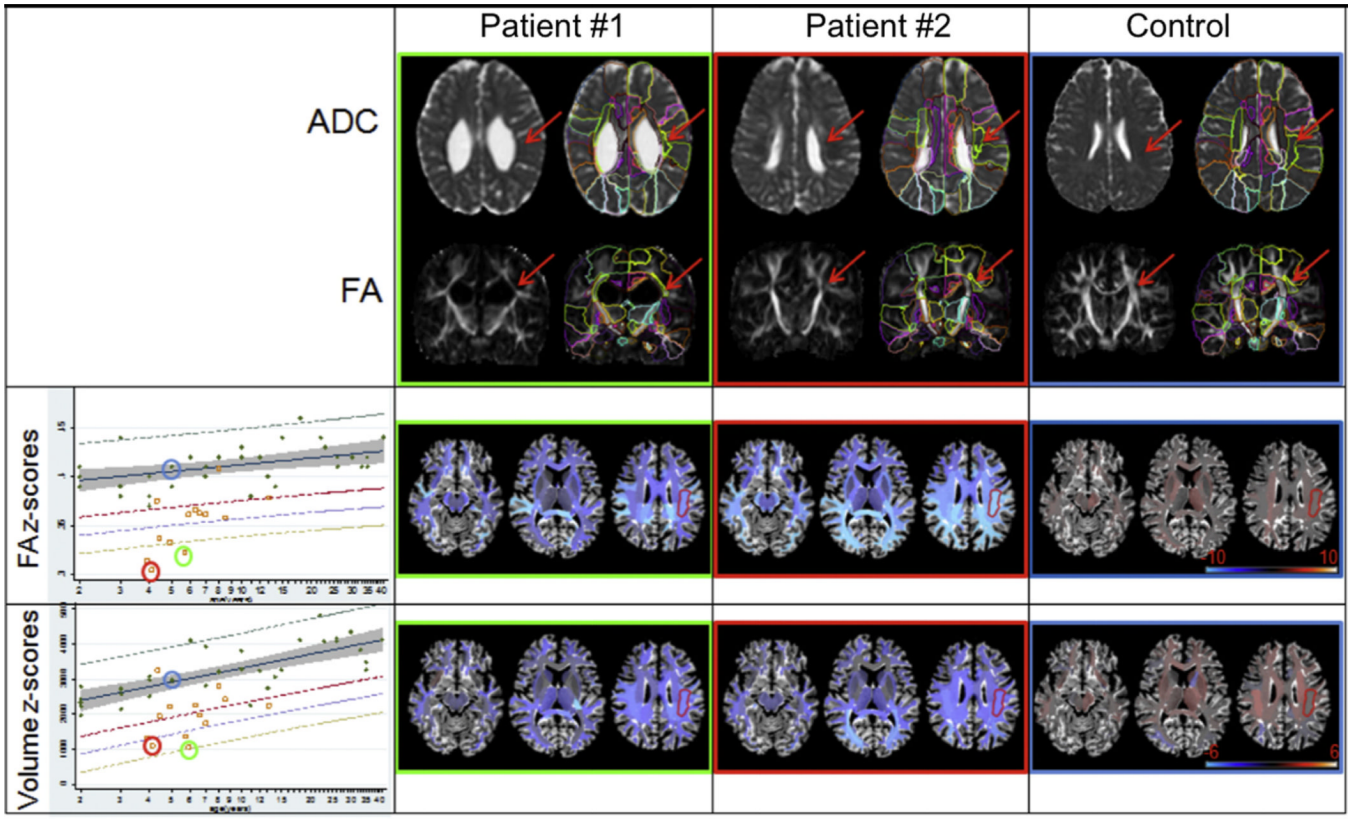


**Fig. 6.**

Demonstration of automated abnormality detection using the atlas enriched by a normal database of developing brains. Color-coding of the second and third row of the right three columns indicates the z-score of the ADC and the FA values in each participant, calculated based on our normal database.

From Faria et al. (2011) with permission.

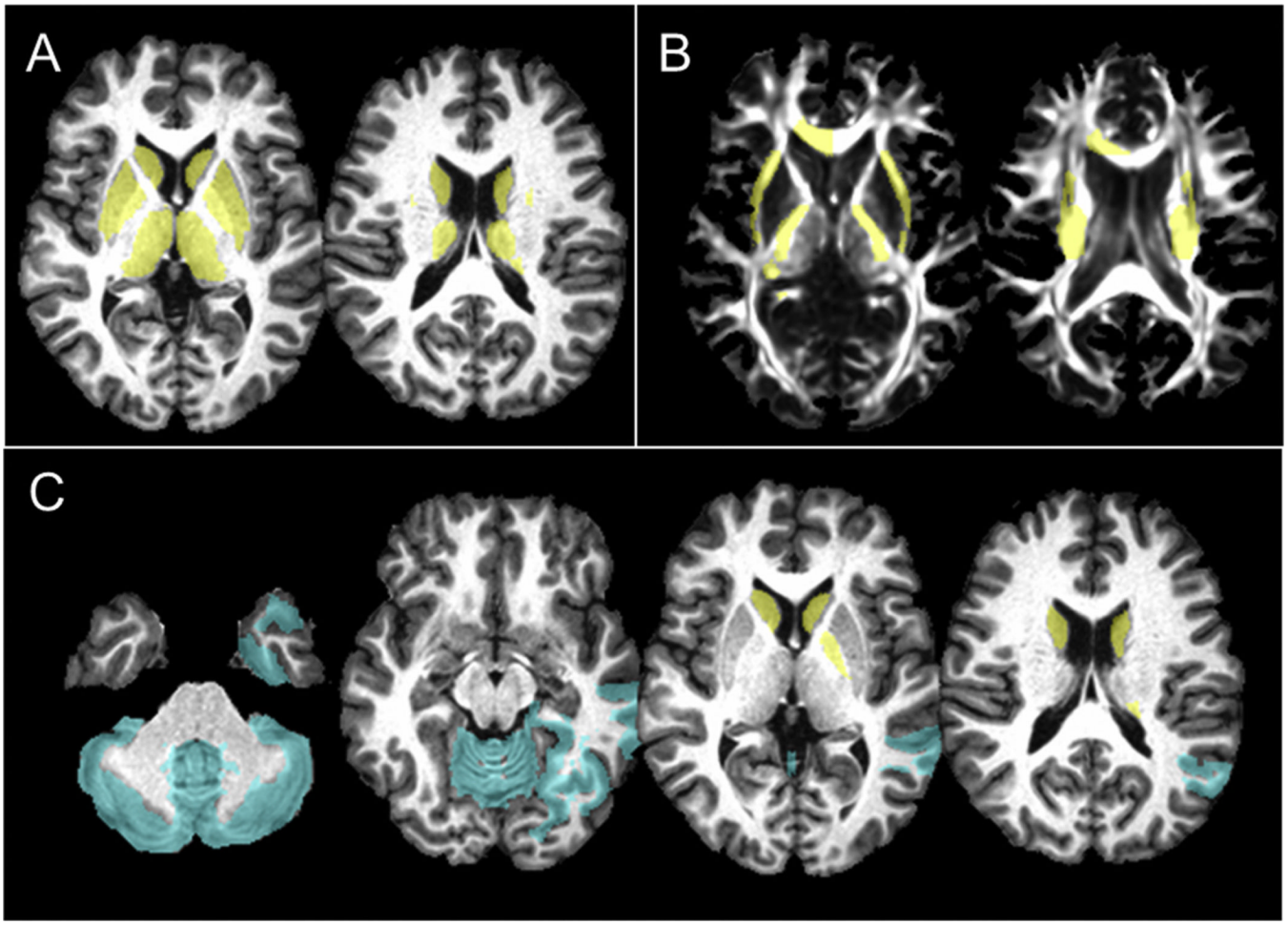


**Fig. 7.**
Volumetric differences between WS and controls. Regions with significant atrophy in WS individuals are highlighted in yellow and those with volumes relatively preserved are blue.

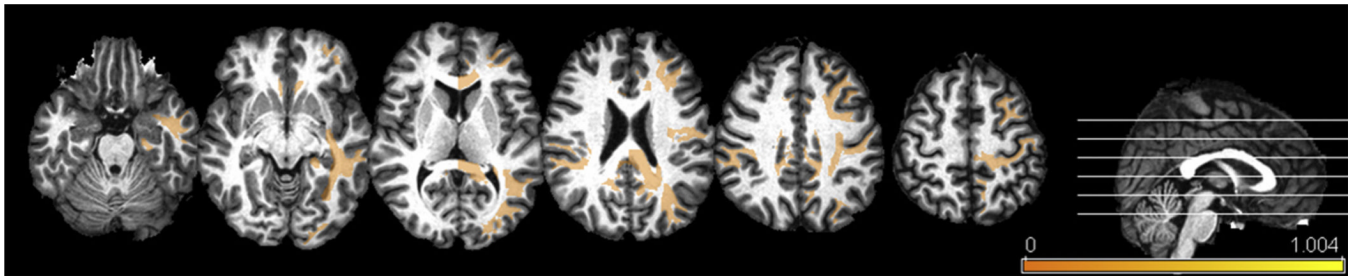


**Fig. 8.**
Regions with a reduction in FA in Rett syndrome ($p$<0.01, uncorrected). Color scale represents ratio of Rett/control.

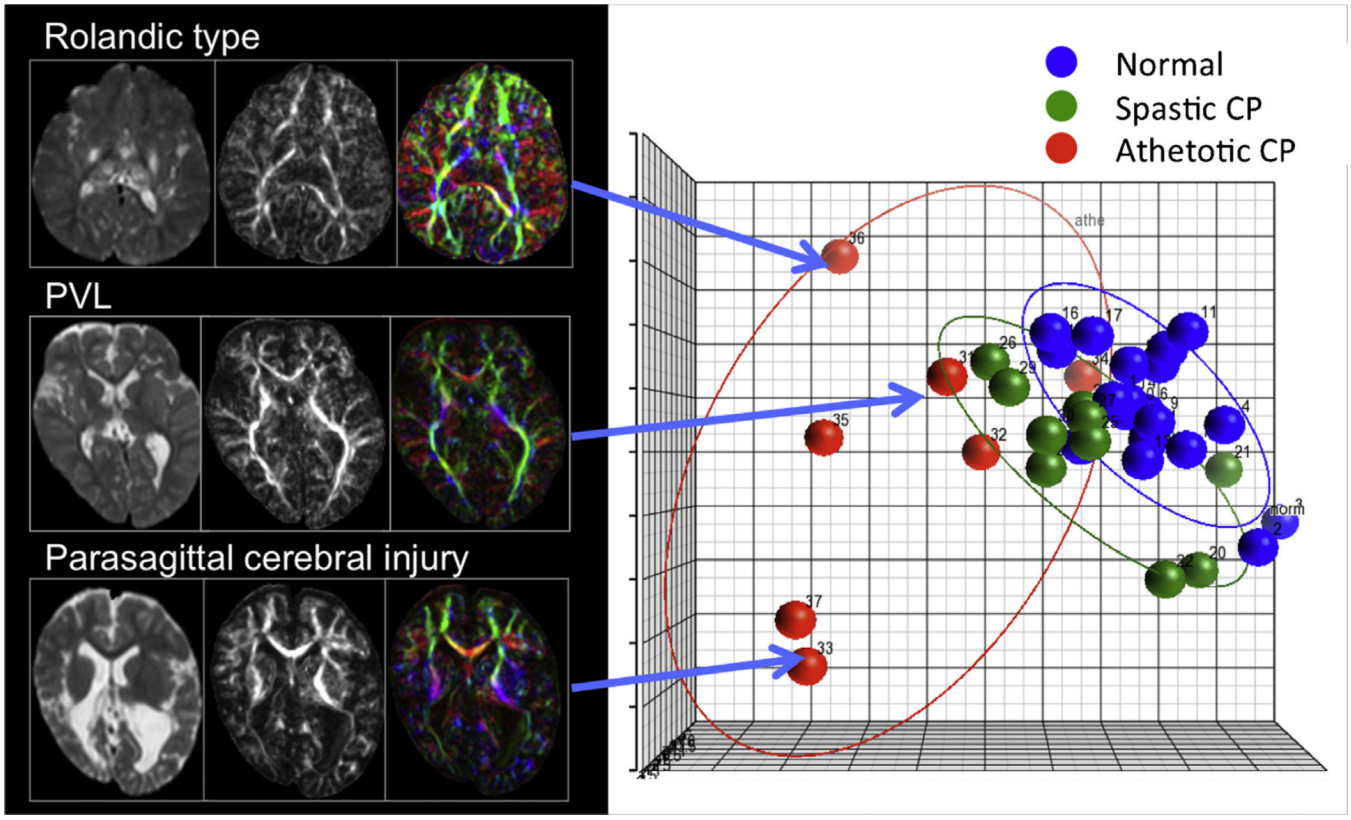


**Fig. 9.**

Multimodal evaluation of two different clinical types of cerebral palsy (CP)(spastic CP and athetotic CP) and a group of normal subjects. The three axes of this scattergram represent the first three principal components extracted by PCA, and a projection of each participant was plotted on this three-dimensional space. The distribution of the control group was the most concentrated among the three groups. The athetotic CP group tended to be more scattered and distant from the normal control group than the spastic CP group. This finding is consistent with the general notion that children with athetotic CP tend to have more severe motor impairment, with more variable accompanying disabilities, than children with spastic CP.

From Yoshida et al. (2013a) with permission.